SELF-SUSTAINED OSCILLATIONS IN DIFFUSERS : MODELLING AND PREDICTIONS

J.-Ch. ROBINET* and G. CASALIS†
ONERA-CERT
2, avenue Edouard Belin, B.P. 4025
31055 TOULOUSE Cedex 4, FRANCE

It has been observed that shock waves in supersonic flow oscillate under certain conditions. These oscillations usually have negative effects especially for flow past transonic airfoils and in supersonic diffusers. It is therefore of practical importance to understand the origin and the consequences of these oscillations. The purpose of this paper is to model and to predict some physical characteristics of self-sustained shock oscillations in transonic diffuser flows. This paper gives first the results of a quasi-one-dimensional stability analysis. The mean flow is calculated with a code solving the averaged Navier-Stokes equations. The present stability approach is however limited to the core region where the viscous effects can be neglected. Furthermore, the quasi-one-dimensional stability approach is generalized in order to study the stability of a two-dimensional mean flow with a small perturbation technique. In order to validate the present approach, the results are compared with Sajben's experimental data and those numerically obtained by Hsieh. As demonstrated below, the main characteristics of the oscillation are clearly obtained: for example the shock motion spectra is correctly reproduced by the present stability approach.

Nomenclature

Latin Alphabet

k	wave number
R_p	exit pressure to total inlet pressure ratio
l	diffuser length (from throat to exit)
h	throat height
U, u	streamwise velocity component
V, v	transverse velocity component
T	temperature
a	sound velocity
t	time
X	amplitude of shock motion

Greek Alphabet

$\omega/2\pi$	frequency
ρ	density

Subscripts

$(.)_o$	upstream value
$(.)_1$	downstream value
$(.)_f$	fluctuation value
$(.)_c$	shock value
$(.)_e$	exit value
$(.)_s$	south boundary value
$(.)_n$	north boundary value

Superscripts

$\bar{(.)}$	mean value

*PhD Student, Department Modelling Aerodynamics and Energetics, Transition and instability Group.

†Research Scientist, Department Modelling Aerodynamics and Energetics, Transition and instability Group.

Introduction

Under certain conditions, the shock wave in supersonic flows may exhibit oscillations. This occurs for example with transonic airfoils and in supersonic diffusers. Different approaches have been used in order to quantify these oscillations and to understand their physical origin. Many experiments have been carried out by Sajben[11] *et al.* in the beginning of 80's whereas some numerical simulations have been tried by Liou, Coakley[9] and Hsieh.[6] A new approach is proposed in this paper which is more theoretical than the two others and which can provide thereby a new insight in this difficult problem. It is more or less admitted that the geometry of the diffuser, the shock intensity, the separation bubble of the boundary layer just downstream the shock and the subsonic core region play an important role in these oscillations. But neither the experiment nor the numerical simulations can explain: "who does what, how and why". The objective is to prove by simple models that the frequency of the self-sustained oscillations at least can be predicted by a small perturbation technique based on inviscid perturbations superimposed to a viscous mean flow.

This first part describes the published results: the experimental and the numerical ones. In the second part, the theoretical aspects of a quasi-one-dimensional stability analysis are described. This approach consists in studying these oscillations using a simple linear stability analysis. This analysis is restricted to the core region where the viscous effects are negligible and, in accordance with experimental results, the mean flow is assumed to be nearly one-dimensional in this region. However, the mean flow is calculated using the code

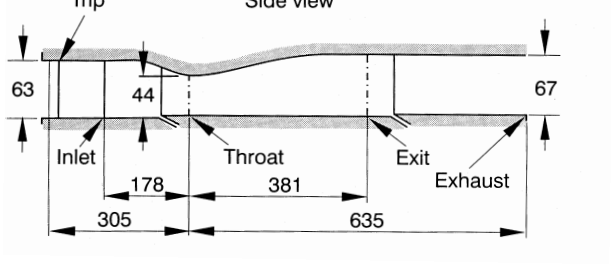

Fig. 1 Sajben *et al.* diffuser model.

FLU3M developed at **ONERA** in order to obtain accurate values for the mean flow. The one-dimensional stability results are then presented in comparison with Sajben's experiments and with Hsieh numerical simulations. In the third part, the quasi-one-dimensionality hypothesis is left in order to study the fully two-dimensional mean flow. The results are finally compared both to experimental results and to the results provided by the previous simplified stability approach.

1 Background of the Present Study

Diffuser Geometry

The major experimental contribution on self-sustained shock oscillations has been brought by the Mc Donnell Douglas team headed by M. Sajben.[1,11,10] One of the diffusers used in the experiment is asymmetric with a flat bottom wall and a converging-diverging channel with a maximum 9^o divergence angle. This diffuser is equipped with many suction slots, so that the flow can be considered two-dimensional, at least in the middle section between the two lateral walls of the channel. Figure 1 gives a sketch of the experimental set-up.

The relative diffuser length is l/h where h is the height at the throat, the length origin is chosen at the throat. In this paper, only the diffuser lengths such as $l/h \leq 13$ are studied with the proposed approaches.

General Descriptions

In this nozzle, the fluid accelerates from subsonic to supersonic speed through a sonic throat, and is abruptly decelerated by a shock-wave located downstream of the throat. The flow in this diffuser is exhausted directly to the ambient air so that the boundary conditions at the exit cross section are closely characterised by a spatially and temporally constant static pressure. The flow conditions are then mainly characterised by the ratio of the static pressure at the exit section to the total pressure at the inlet: $R_p = p_e/p_t$. This ratio determines, among other properties, the shock strength and the upstream Mach number M_0. The flow patterns obtained with this diffuser depend on the Mach number. In Sajben's experiment, shock-induced separation occurs for Mach numbers M_0 greater than 1.3 and, in this case spontaneous self oscillations have been observed. These gether with the occurrence of fluctuations downstream of the shock. In all cases, no oscillation has been observed in the supersonic zone. The following results are limited to one value of R_p : $R_p = 0.72$ ($M_0 = 1.34$).

Experimental and Numerical Results

Among the Sajben's experimental results, the shock motion power spectrum is of particular interest. This spectrum[1] is represented in figure 2.

It shows that the most sensitive frequencies, for a

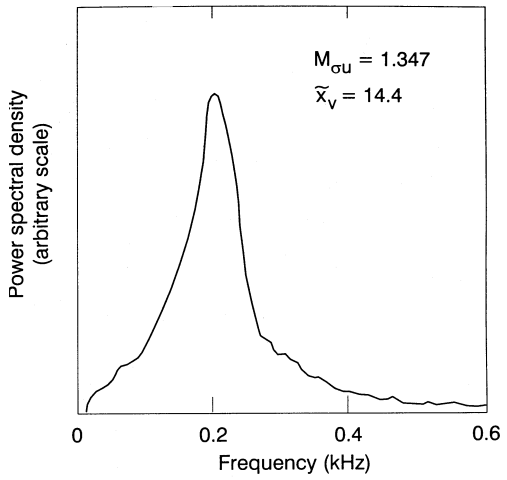

Fig. 2 Shock motion power spectrum, experiment.

diffuser length $l/h = 14.4$, are close to 200 Hz. Different lengths ($12 \leq l/h \leq 30.5$) have been studied by Sajben *et al.*[11] Computations have been performed by Coakley, Liou and Hsieh,[8,9] for the same diffuser configuration. These simulations consisted in solving the unsteady averaged Navier-Stokes equations with a classical turbulence model. They were achieved in two steps: steady computations provided the mean flow and then the unsteady computations determined the fluctuating quantities. These unsteady computations have been realised by imposing a fluctuating pressure at exit section. Hsieh and Coakley[6] used different diffuser lengths (see Table 1).

Frequency (Hz)	l/h (*case*)
300	8.66 (A)
250	10.06 (B)
210	12.08 (C)
310	14, 7 (D)

Table 1 Oscillation frequency for different diffuser lengths (numerical results).

Figure 3 shows the computed shock motion power spectrum corresponding to these cases. It can be observed that when the diffuser length l/h is less than 12 the frequency of oscillation reduces from 300 to 210 Hz as the downstream boundary location varies

creases to 310 Hz for the greatest length ($l/h = 14.7$). The latter does not agree with the experimental result (198 Hz) published by Sajben[11] and given in figure 2.

Taking into account all these published results (exper-

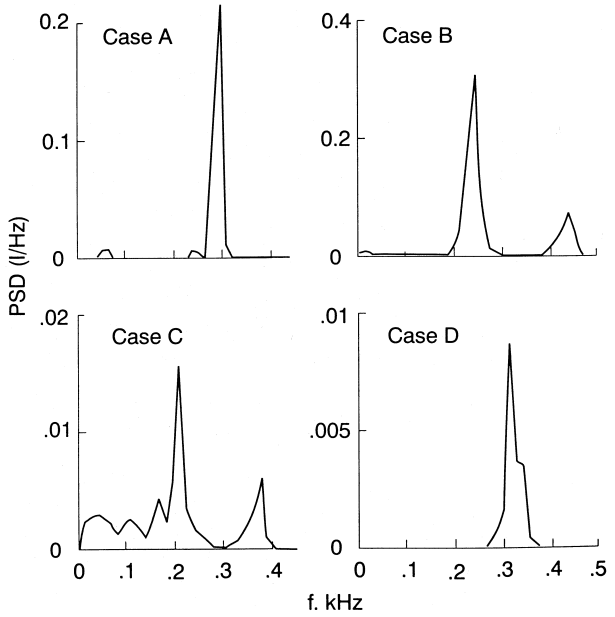

Fig. 3 Shock motion power spectrum, Computation

iment and numerical simulations), the present analysis is devoted to a simpler and more analytical approach. Let us summarize, the different diffuser lengths used in the Sajben's experiment, in Hsieh's calculation and in our present approach:

- Sajben's experiment: $12 \leq l/h \leq 30.5$
- Hsieh's simulation: $8.6 \leq l/h \leq 14.7$
- present approach: $8.6 \leq l/h \leq 13$

2 Mean and Fluctuating Flows

The purpose of this section is to describe the main assumptions employed in the proposed small perturbation technique. The classical coordinate system (x, y) is used, where x is the streamwise coordinate and y is perpendicular to it.

Small Perturbation Technique

Two present approaches are based on the standart small perturbation technique. The instantaneous flow is written as the superposition of a basic flow and of a small fluctuation. All physical quantities q (velocity, pressure, ...) are thus decomposed into a mean value and a fluctuating one :

$$q = \bar{q} + q_f. \qquad (1)$$

The physical quantities related to the mean flow are overlined; for example, $\bar{U}$ is the mean streamwise

Mean Flow Calculation

The mean flow comes from a computation. The code **FLU3M**[2] developed at **ONERA** solves the averaged Navier-Stokes equations, a classical $k - \varepsilon$ model has been used. This computation is similar in principle to the first step of the numerical simulation done by Liou *et al.*. Before describing the formalism of the proposed model, we must first check that the computed mean flow is in agreement with Sajben's experimental results.

The two different grids has been used for the computation of the mean flow. The first one consists in a (136x99) grid with a fine distribution of points only near the upper and lower walls in order to have enough points in the boundary layers. In the x direction, the mesh is strengthened around the expected shock wave location. The second computational grid (136x111 points) is refined in the y-direction in the central zone of the diffuser in order to compute the evolution in the y-direction of mean flow more accurately. Figures 5 and 6 show the ex-

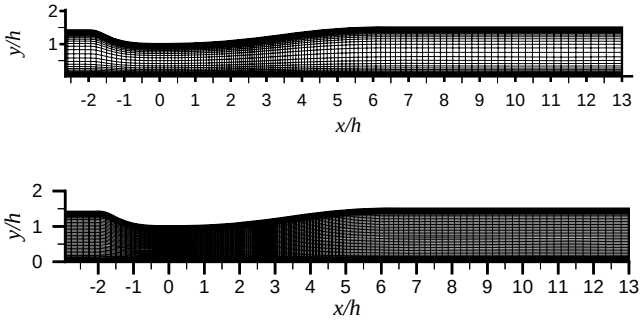

Fig. 4 The two different grids

perimental and numerical results respectively for the iso-$\bar{U}$ contours. From these results, it can be concluded that both computed mean flows are in good agreement with the experimental data. However, a detailed study shows that small differences still exit just downstream of the shock and between the y-derivative of the different mean flow quantities.

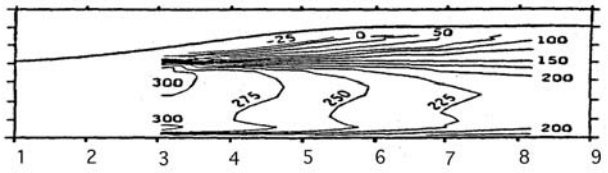

Fig. 5 $\bar{U}$ contours (m/s), experiment

An instructive behaviour is provided by the evolution of the longitudinal mean velocity in the x direction (and in the middle of the core flow), see figure 7. It can

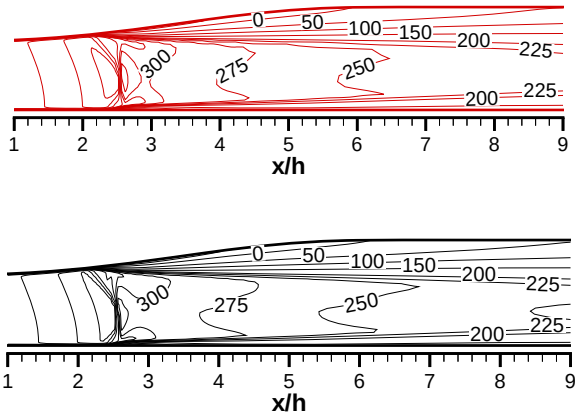

Fig. 6 $\bar{U}$ contours (m/s), computation. Top : (136x99) points, bottom : (136x111) points

be observed that instead of a continuous decrease up to exit section, the mean flow increases just downstream of the shock before to decrease. This local convergent effect results from the large separation bubble in the upper boundary layer. And since many years, it is well known that the shock is unstable in a converging nozzle (i.e. when the flow accelerates).[7]

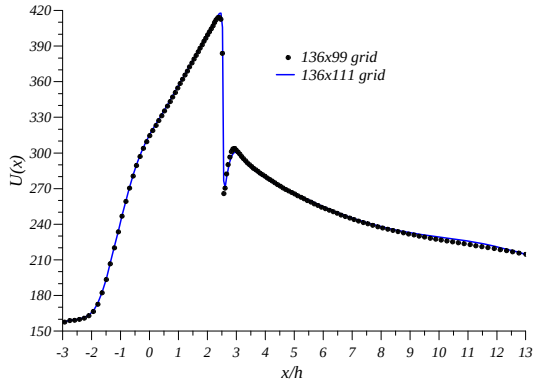

Fig. 7 Mean flow evolution, core flow.

It must be pointed out that consequently the proposed approachs will take into account the separated region, but only through the mean flow values. So in these approaches, the boundary layer and its separated region are considered as steady.

Basic Equations for the Small Perturbation Technique

The equations for the instantaneous flow are the Euler equations, the energy equation written for the total enthalpy and the equation of perfect gas. The proposed approaches are thus limited to the core region where the viscous effects can be neglected.

- Equation of continuity:

$$\frac{\partial \rho}{\partial t} + \frac{\partial (\rho U)}{\partial x} + \frac{\partial (\rho V)}{\partial y} = 0, \tag{2}$$

$$\rho \frac{\partial U}{\partial t} + \rho U \frac{\partial U}{\partial x} + \rho V \frac{\partial U}{\partial y} + \frac{\partial P}{\partial x} = 0, \tag{3}$$

- y-momentum equation :

$$\rho \frac{\partial V}{\partial t} + \rho U \frac{\partial V}{\partial x} + \rho V \frac{\partial V}{\partial y} + \frac{\partial P}{\partial y} = 0, \tag{4}$$

- Enthalpy equation :

$$\rho \frac{\partial h_i}{\partial t} + \rho U \frac{\partial h_i}{\partial x} + \rho V \frac{\partial h_i}{\partial y} = \frac{\partial P}{\partial t}, \tag{5}$$

- Total enthalpy definition :

$$h_i = C_p T + \frac{U^2 + V^2}{2}, \tag{6}$$

- Equation of state :

$$P = r \rho T, \tag{7}$$

where r and C_p are respectively the perfect gaz constant ($r = 287\ m^2 s^{-2} K^{-1}$) and specific heat coefficient ($C_p = 1007\ m^2 s^{-2} K^{-1}$).
The instantaneous flow is also solution of the Rankine-Hugoniot relations written at the instantaneous location of the shock :

$$\rho_1 \left(V_{n1} - W_c\right) = \rho_0 (V_{n0} - W_c), \tag{8}$$

$$P_1 + \rho_1 (V_{n1} - W_c)^2 = P_0 + \rho_0 (V_{n0} - W_c)^2, \tag{9}$$

$$V_{\tau 1} = V_{\tau 0}, \tag{10}$$

$$C_p T_1 + \frac{1}{2}(V_{n1} - W_c)^2 = C_p T_0 + \frac{1}{2}(V_{n0} - W_c)^2, \tag{11}$$

where V_n is the velocity component normal to the shock, V_τ is the tangential component and W_c is the velocity of the shock front.

3 Stability Analysis

The decomposition (1) is firstly introduced in equations (2) to (7). The mean flow, which satisfies the Navier-Stokes equations, is assumed to be a solution of the inviscid equations in this region. The resulting equations are further simplified by considering that the perturbation is small, so that the nonlinear fluctuating terms can be neglected.
Finally, equations (2) to (7) are transformed into a linear system, the coefficients of which are functions of the mean flow.

Perturbation Form

In this part an additional assumption is used, which will be not considered in section 4. According to the experimental and numerical results, the mean flow in the core region is assumed to be weakly dependent on y, so that any mean quantity verifies the relation :

$$\partial\bar{q}/\partial y \ll \partial\bar{q}/\partial x, \qquad \forall x, \forall y. \tag{12}$$

With this assumption, the perturbation can be seeked with a uniform exponential dependence with respect to y. Thus any fluctuating quantity is written as :

$$q_f(x,y,t) = \Re\left[q(x).e^{\omega_i t}.e^{i(ky-\omega_r t)}\right], \tag{13}$$

where q is a complex function, k is a real wave number and ω_i is a temporal amplification rate, whereas the real part ω_r of ω characterises the frequency of the perturbation. $\Re(z)$ is the real part of z. The linear stability of the flow depends on the sign of ω_i: for $\omega_i < 0$ the mean flow is linearly stable, whereas for $\omega_i > 0$ the mean flow is unstable.

Stability Equations and Boundary Conditions

With the perturbation (13), the linearized Euler equations become an ordinary fourth-order differential system :

$$\mathbf{C}\frac{d\mathbf{Z}}{dx} = \mathbf{B}\mathbf{Z}, \tag{14}$$

where $\mathbf{Z}(x)$ is the amplitude function vector of the perturbation. Its components are T, ρ, u, v, which denote respectively the fluctuating temperature, the density and the longitudinal and transverse velocities components. $\mathbf{C}$ and $\mathbf{B}$ are two $(4,4)$ complex matrices which are functions of the mean flow and of the coefficients ω and k.[4]

In all the tested experimental configurations, no fluctuation has been observed in the supersonic zone flow. For this reason, the first boundary condition is chosen as :

$$\mathbf{Z}(0) = 0, \tag{15}$$

This means that there is no fluctuation at the throat. In exit section, the fluctuations do not necessarily vanish. It is only imposed that the perturbations are bounded at the exit section:

$$\|\mathbf{Z}(l/h)\| \ll \infty. \tag{16}$$

Eigenvalue Problem

The differential system (14)-(16) has $\mathbf{Z} \equiv 0$ as natural and trivial solution. Moreover it is the only one unless the problem becomes singular. In fact, the determinant of the matrix C is always invertible except at the position defined by $\bar{M} = 1$. The problem is thus regular from throat to shock. Then, according to the boundary condition (15), $\mathbf{Z} \equiv 0$ is the only solution of supersonic zone there is no fluctuation. However, if the system of equations (14) is singular at the mean shock position, another solution (i.e. not trivial) may exist. To find this solution, a special procedure needs to be used at the shock position. This procedure is obtained with the shock relations (8) to (11).

Linearised Shock Relations

According to the small perturbation technique (1) and to expression (13), the perturbed position of the shock is written as :

$$x = \bar{x}_c + \Re\left[Xe^{i(ky-\omega t)}\right]. \tag{17}$$

In (17), $\bar{x}_c$ represents the mean shock position and X the amplitude of the shock displacement which is assumed to be a small quantity. The Rankine-Hugoniot equations (8) to (11) are then linearized by performing a first order Taylor expansion with respect to X. The quantities downstream of the shock are denoted by subscript 1 and those upstream of the shock by subscript 0. In fact, all quantities q (q_1 or q_0) are the sum of the mean and of the fluctuating values evaluated just downstream for (q_1) or upstream for (q_0) of the perturbed position of the shock:

$$q(x,y,t) = \bar{q}(\bar{x}_c + XE) + q_f(\bar{x}_c + XE),$$

where $E = e^{i(ky-\omega t)}$.
After expansion, q_1 is written as :

$$q_1(x,y,t) = \bar{q}_1(\bar{x}_c) + \frac{\partial\bar{q}_1}{\partial x}(\bar{x}_c)XE + q_1(\bar{x}_c)E.$$

As there is no fluctuation upstream of the shock, q_0 is simply given by:

$$q_0(x,y,t) = \bar{q}_0(\bar{x}_c) + \frac{\partial\bar{q}_0}{\partial x}(\bar{x}_c)XE.$$

It can be noted that in the previous expression the derivative of q_0 with respect to x corresponds to the left derivative (in x_0^-); the same is true with the x-derivative of q_1 and the right derivative (in x_0^+). After some calculation, the linearized shock relations lead to an algebraic system of equations:

$$A\mathbf{Z}(\bar{x}_c) = \xi X, \tag{18}$$

where $\mathbf{Z}(\bar{x}_c)$ is the vector of the fluctuating amplitudes calculated at $\bar{x}_c$, ξ is a complex vector and A is a fourth-order complex matrix; A and ξ are known. From another point of view, it should be noted that the behaviour of mean flow on both sides of shock (for example : the local convergent effect indicated in figure 7) occurs in the term ξ through the right and left derivatives of the mean flow. Finally, as the matrix A is invertible,[4] the vector $\mathbf{Z}$ at the mean shock position is known:

$$\mathbf{Z}(\bar{x}_c) = A^{-1}X\xi. \tag{19}$$

the shock oscillation amplitude X, which cannot be determined within the linear stability analysis.

Summary

The stability problem has been easily solved in the supersonic zone, $\mathbf{Z} = 0$ is the unique solution. In the subsonic zone, the system (14) with the boundary conditions (15) and (16) is an eigenvalue problem. The trivial solution $\mathbf{Z} \equiv 0$, $X = 0$ is a solution. A non-zero solution can exist only if the problem is singular, which implies a particular choice of the wave number k and of the complex circular frequency ω of the perturbation. This choice corresponds to a dispersion relation between these numbers, which cannot be determined analytically. In the following, a numerical procedure devoted to this point is described.

Analytical study

If the mean flow is considered as uniform i.e. independent of x, the differential system (14) becomes a linear differential system with constant coefficients. Then an analytical solution can be calculated:

$$\mathbf{Z}(x) = \sum_{j=1}^{4} c_j \mathbf{Z}_j(x) \text{ with } \mathbf{Z}_j(x) = \mathbf{V}_j e^{l_j x}, \qquad (20)$$

where the coefficients c_j are unknown integration constants, which will be determined by the boundary conditions. l_j and $\mathbf{V}_j$ are respectively the eigenvalues and eigenvectors of matrix $\mathbf{C^{-1}B}$, see (14) . The expressions of l_j and $\mathbf{V}_j$[4] are given in the appendix. Physically, the first two modes ($j = 1, 2$) correspond to the acoustic modes, respectively the downstream and upstream travelling waves, and the other two modes ($j = 3, 4$) correspond to the entropic and the rotational modes which are convected with the mean flow. In order to verify the condition (16), these different modes $\mathbf{V}_i e^{l_i x}$ cannot exhibit an exponentially increasing behaviour: $\Re(l_i) \leq 0$ where $\Re(l_i)$ denotes the real part of l_i. It can be shown that $\Re(l_3) \leq 0$ if $\omega_i \geq 0$, $\Re(l_2) \leq 0$ and $\Re(l_1) \geq 0$ for all ω and k. Nevertheless, when $\omega_i \leq 0$, $\mathbf{V}_3 e^{l_3 x}$ and $\mathbf{V}_4 e^{l_3 x}$ are smaller than $\mathbf{V}_2 e^{l_2 x}$, it can be then considered that the only one not acceptable mode with respect to boundary condition (16) is $\mathbf{V}_1 e^{l_1 x}$. The relation $c_1 = 0$ must be imposed. This relation amounts to suppose that there are no downstream travelling waves; this is finally in agreement with Culick and Rogers's theory.[5] According to the latter, the reflected downstream travelling wave amplitude is about 6 times smaller than the upstream travelling wave amplitude (in the case of the mean flow described in section (2)). The general solution is written as :

$$\mathbf{Z}(x) = c_2 \mathbf{Z}_2(x) + c_3 \mathbf{Z}_3(x) + c_4 \mathbf{Z}_4(x), \qquad (21)$$

the presence of any uniform zone, but, at a certain distance from the shock, it is assumed that the mean flow does not depend too much on x. In this "uniform zone", for $x \geq x_u$ ($x_u/h \simeq 11$), the solution of (14) can be written as (21). Equation (14) is then numerically integrated for each vector $\mathbf{Z_j}$ (j=2,3,4) by decreasing values of x from the uniform zone boundary x_u up to the mean shock position $\bar{x}_c$. At this position, there are two formulations of $Z(x)$; the first one comes from the numerical integration and equation (21) and the second one is simply given by the boundary condition (19). These two expressions should coincide. For a given circular frequency ω_r, the unknowns are the complex constants c_2, c_3, c_4. These six real unknowns are searched in order to verify the following relationship :

$$\mathbf{Z}(\bar{x}_c) = c_2 \mathbf{Z}_2(\bar{x}_c) + c_3 \mathbf{Z}_3(\bar{x}_c) + c_4 \mathbf{Z}_4(\bar{x}_c),$$

which provide four scalar complex relations. A non zero solution only can exist if the rank of this system of four relations is only three. This condition is a dispersion relation: it is satisfied with a particular value of (k, ω_i) for a given value of frequency $\omega_r/2\pi$ of the perturbation. A trial and error method is finally used to determine the eigenvalues with an initial guess for (k, ω_i).[3,4] Table 2 below gives the eigenvalues (k, ω_i) for the fixed frequency 200 Hz. These results have been obtained with the mean flow calculated for the diffuser length $l/h = 13$.

k (m^{-1})	$\omega/2\pi = (\omega_r + i\omega_i)/2\pi$
136x99 grid	
-5.002	$200.000 - 3.740i$
-4.839	$200.000 - 98.867i$
136x111 grid	
-5.024	$200.000 + 3.834i$
-4.836	$200.000 - 98.852i$

Table 2 Numerical stability results.

Two modes seem to be solutions of the stability problem. Nevertheless, only the second one, the mode $(200 - 98.86i)$, will be considered hereafter because the first mode, $(200 - 3.74i)$ is very dependent of the computational grid.

Computation of Shock Motion

As explained before, the fluctuations are proportional to the shock amplitude X. In order to determine a spectrum from the stability results, a normalisation must be introduced for the amplitude functions. The fluctuating pressure at the exit section has been chosen for that purpose as it is done with the numerical simulations. As the fluctuating pressure spectrum is not known at the exit section, a uniform law is simply imposed :

$$|p_f(x_e)|_{rms} = \varepsilon \bar{P}(x_e), \qquad (22)$$

sure at the exit section is hence given as a constant part of the mean pressure.

Results

In order to validate the quasi-one-dimensional stability theory, the results are first compared with Sajben's experimental values and Hsieh's computations. The stability of the mean flow is then examined.

- **Shock Motion Spectra**

Figure 2 shows the experimental shock motion spectrum. It exhibits a well-defined peak close to 200 Hz, this means that the shock is more sensitive to excitations of frequencies around 200 Hz. The shock motion spectrum calculated by the one-dimensional stability analysis also provides a peak close to 200 Hz. Figure 8 presents this result. This spectrum has been calculated for the $l/h = 13$ diffuser length and the mean flow calculated with the (136x111) grid. In order

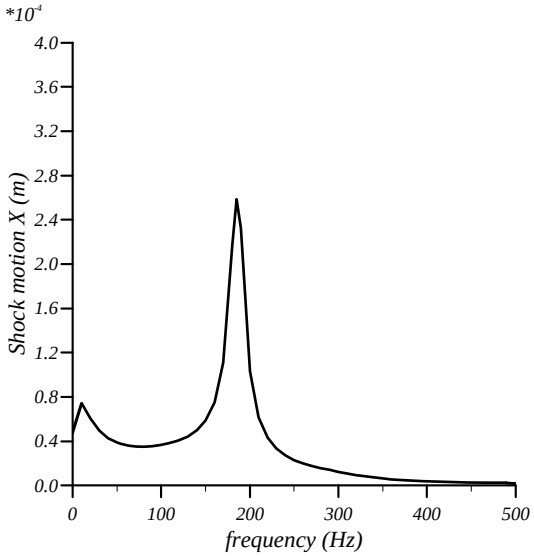

Fig. 8 Shock motion spectrum, $l/h = 13$.

to evaluate the robustness of this encouraging result, the stability analysis has been performed again but with the mean flow calculated with the (136x99) grid. Furthermore, just for the stability analysis, a narrow mesh in x (180 points instead of 136) has been tested using a Tchebicheff polynomial interpolation for the mean flow. Figure 9 shows that the stability results do not depend neither on the grid used for the stability nor on the grid used for the computation of the mean flow. Concerning approximation (12), the shock motion spectra must be more or less independent of y. Figure 10 confirms this behaviour where j represents the vertical index for the y-line of the mesh. It seems that the quasi-one-dimensional stability theory can be applied for Sajben's experiment.

One fundamental parameter in the determination of the self-sustained oscillations frequency is the length

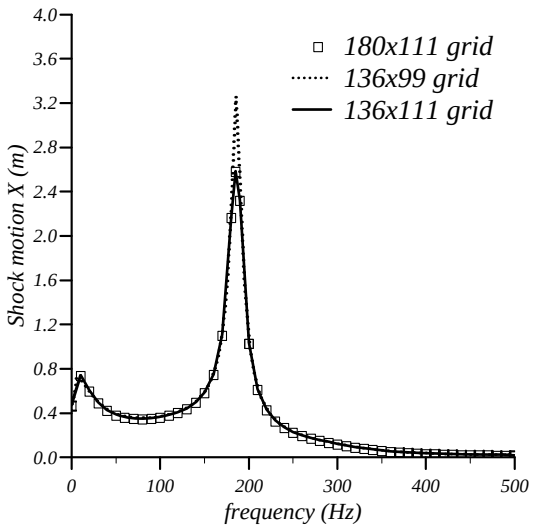

Fig. 9 Robustness of shock motion spectrum.

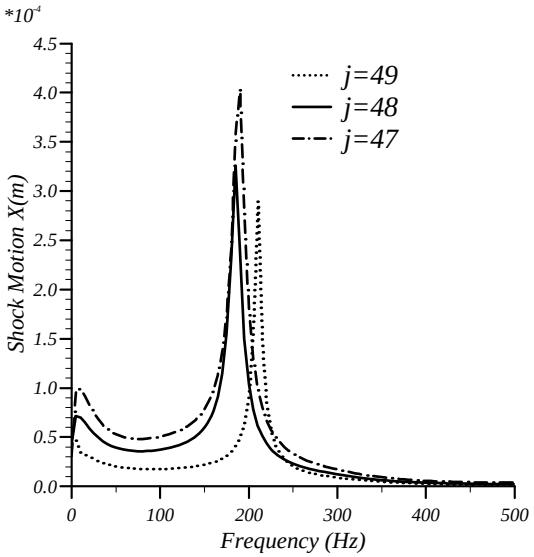

Fig. 10 y-dependence of shock motion spectrum.

of the diffuser. Different stability analyses have been performed for different lengths. Figure 11 shows the evolution of the observed frequency peak in the shock displacement spectra versus the diffuser length. For a diffuser length such as $l/h = 13$, the one-dimensional stability theory seems to be in good agreement with the experimental and numerical results. The four points with the label "computation" have been extracted from figure 3.[6]

- **Evolution of ω_i with the Frequency**

The main objective of a linear stability analysis is to determine if the basic flow is stable with respect to infinitesimal perturbations. This stability is characterised by the sign of the temporal amplification growth rate ω_i. Figure 12 shows the evolution of the temporal amplification coefficent ω_i, it is always negative whatever the frequency is. Therefore, according to

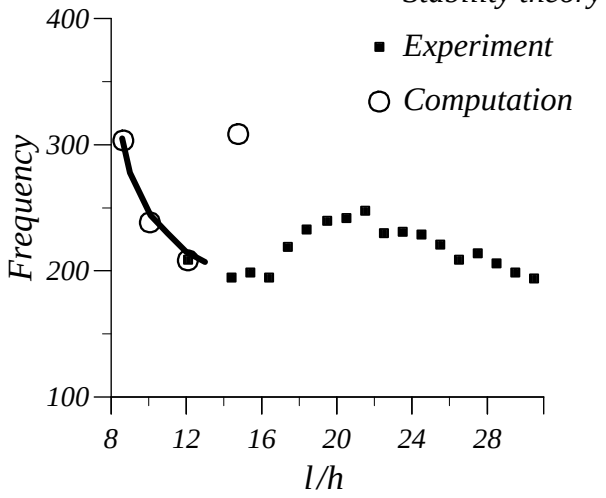

Fig. 11 Frequency versus diffuser length.

the stability definition, the mean flow is stable. Thus if the mean flow could be strictly not perturbed (at the exit section by some pressure fluctuations), no shock oscillation and no perturbation in the downstream zone could be observed. This could be verified experimentally by adding a second throat close to the exit section in order to eliminate any downstream excitation.

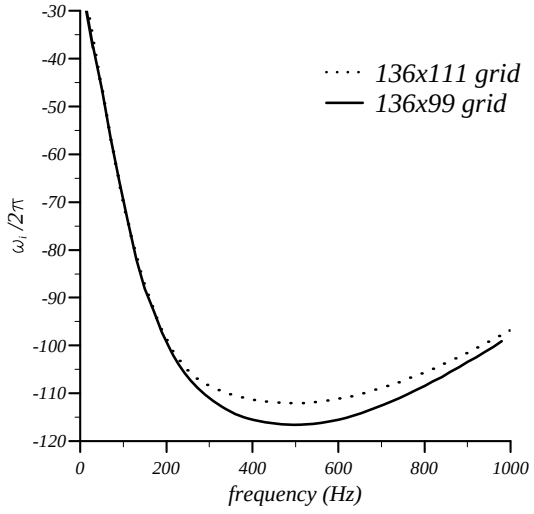

Fig. 12 Variation of ω_i.

4 Two-dimensional Analysis

This section is devoted to the extension of the previous stability analysis. A two-dimensional approach is applied again to Sajben's diffuser in order to validate it in comparison with the previous one.

Small Perturbation Equations

If the mean flow is fully two-dimensional, depending on x and y, the assumption (12) is no longer valid. written as (13). In this case, the fluctuating quantities are expressed by :

$$q_f(x,y,t) = \Re\left[q(x,y).e^{\omega_i t}.e^{-i\omega_r t}\right], \qquad (23)$$

where $q(x,y)$ is a complex function. In the present two-dimensional study, the temporal amplification rate ω_i is set equal to zero.
The linearized Euler equations then become a fourth-order partial differential system :

$$\mathbf{C}\frac{\partial \mathbf{Z}}{\partial x} + \mathbf{D}\frac{\partial \mathbf{Z}}{\partial y} = \mathbf{B}\mathbf{Z}, \qquad (24)$$

where $\mathbf{C}$, $\mathbf{D}$ are real (4x4) matrices and $\mathbf{B}$ is complex (4x4) matrix, see appendix.

Two-dimensional Shock Relations

By a method similar to that described in section 3, the fluctuating quantities can be calculated at the mean shock position.
The perturbed shock position is written as :

$$x = \bar{x}_c + \Re\left[X(y)e^{-i\omega t}\right], \qquad (25)$$

where $X(y)$ is a complex function which represents the amplitude of the shock displacement. As in the one-dimensional analysis, the Rankine-Hugoniot relations are linearized with respect to X. After expansion, the fluctuating quantities at the mean shock position can be expressed as :

$$\mathbf{Z}(\bar{x}_c) = \mathbf{A}^{-1}\left(\xi X + \eta\frac{dX}{dy}\right) \qquad (26)$$

ξ and η are complex vector functions of the downstream mean flow and ω, see appendix.
Finally, with a similar procedure to the one described in 3, the shock motion can be computed by imposing the fluctuating pressure at exit section.

Computational Domain

The choice of this computational domain is principally imposed by the limitation of the theory. The stability theory being an inviscid theory, the boundary layers are out of the scope of this study. The computational domain has been chosen in the core flow, with a rectangular cartesian grid interpolated by the Tchebicheff polynomials from the original grid (136x111). Figure (13) shows this computational domain (black rectangle). The dimension of the domain

Fig. 13 Two-dimensional computational domain.

is :

$$\begin{aligned}\mathcal{D} &= ([\bar{x}_c/h, x_e/h] \times [y_s/h, y_n/h]) \\ &= ([2.61, 13] \times [0.3, 0.6]).\end{aligned} \qquad (27)$$

The system (24) is of first-order in x and in y. In order to close the partial differential equations system, two boundary conditions must be introduced. The first condition is the values of the fluctuating quantities at the mean shock position (26). The second one is the main difficulty of this $2D$ approach. A homogeneous Neumann condition has been finally imposed on the lower boundary of the domain:

$$\frac{\partial \mathbf{Z}}{\partial y} = 0 \tag{28}$$

Results: Shock Motion Spectrum

Figure 14 shows the shock motion spectrum in the core flow (median line: $j = 56$). The proposed

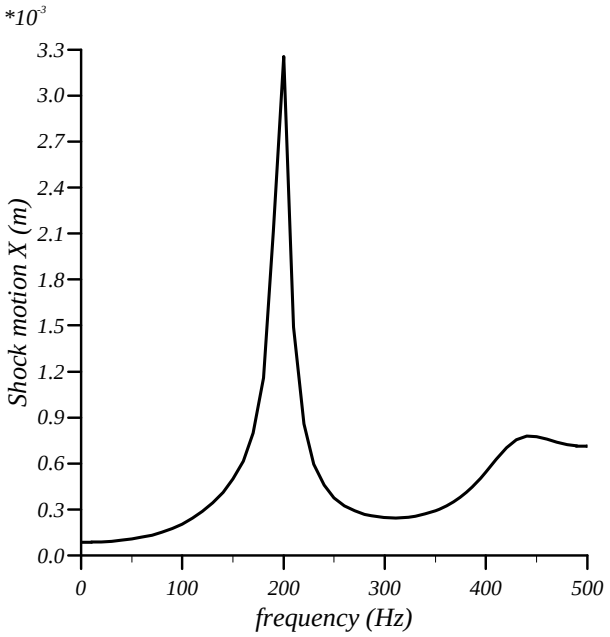

Fig. 14 Shock motion spectrum.

two-dimensional approach seems thus to be in good agreement with the experimental results, the results exhibit a peak close to 200 Hz. The results of this two-dimensional analysis must be independent of the grid and of the dimension of the computational domain. To check this assumption, two different grids have been chosen. For domain $\mathcal{D}$, two different grids have been used: (80x30) points and (80x40) points. Figure 15 shows the shock motion spectrum for these different grids. It can be seen that the grid doesn't influence the results too much. The characteristic frequency is clearly obtained with these two grids, only a difference is perceptible on the amplitude of the shock displacement at 200 Hz.

Summary and Conclusions

The goal of this paper is to present two new approaches based on the small perturbation technique in order to explain and to predict the self-sustained

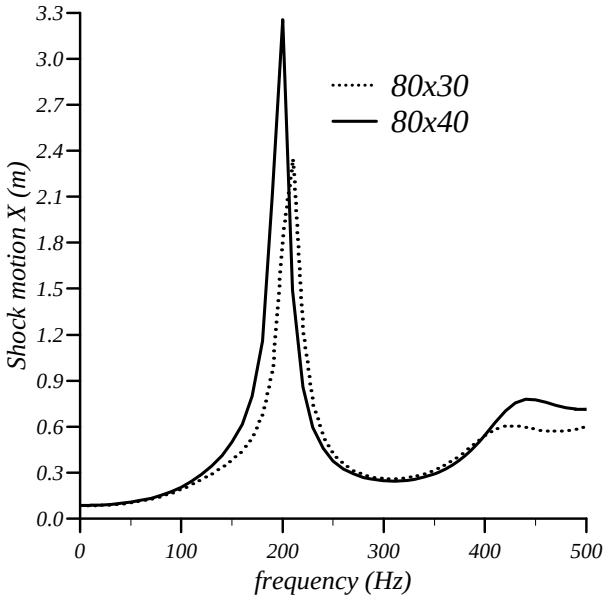

Fig. 15 mesh sensitivity.

shock oscillations observed in many diffusers: a $1D$ linear stability theory and a $2D$ computation.
In the Sajben's diffuser, the mean flow in the core region can be considered as a quasi-one-dimensional flow. Then an appropriate stability analysis has been developed in order to try to understand and to predict the self-sustained oscillations origin. The comparisons between experimental data, numerical simulations and linear theory have shown that the latter can provide the frequency of the shock oscillations. Finally, this study can give some new insight into the physical origin of the observed self-excited shock oscillations. Indeed, this analysis can show that at least in some cases, self-sustained shock oscillations can be explained and predicted with an inviscid linear stability theory but with a mean flow computed with Navier-Stokes equations.

Acknowledgements

This study has been carried out under contract $n^o 93/CNES/3040$ granted by the French Centre National d'Etudes Spatiales (CNES). The mean flow has been computed by R. Hallard (**ONERA**).

References

[1]T. J. Bogar, M. Sajben, and J. C. Kroutil. Characteristic Frequencies of Transonic Diffuser Flow Oscillations. *AIAA Journal*, Vol. 21, No. 2, pp. 1232-1240, 1983.

[2]L. Cambier, D. Darracq, M. Gazaix, Ph. Gullien, Ch. Jouet, and L. Le Toullec. Améliorations récentes du code d'écoulements compressibles FLU3M. Progress and Challenges in CFD Methods and Algorithms, AGARD-CP-578, April 1996.

[3]G. Casalis, R. Hallard, Ch. Jouet, and J.-Ch. Robinet. Calcul des caractéristiques stationnaires et instationnaires d'un écoulement décollé dans une tuyère, cas bidimensionnel. Convention CNES 933040, ONERA, Septembre 1996.

Transonic Diffuser Flows. *Aerospace Science and Technology*, Vol. 1, No. 1, pp. 37-47, 1998.

[5]F. E. C. Culick and T. Rogers. The Response of Normal Shocks in Diffusers. *AIAA Journal*, Vol. 21, No. 10, pp. 1382-1390, 1983.

[6]T. Hsieh and T. J. Coakley. Downstream Boundary Effects on the Frequency of Self-Excited Oscillations in Diffuser Flows. *AIAA paper 87-0161,* jan., 1987.

[7]A. Kantrowitz. The Formation and Stability of Normal Shock Waves in Channel Flows. Technical note 1225, NACA, March 1947.

[8]M. S. Liou and T. J. Coakley. Numerical Simulation of Unsteady Transonic Flows in Diffusers. *AIAA Paper 82-1000,* june, 1982.

[9]M. S. Liou, T. J. Coakley, and M. Y. Bergmann. Numerical Simulation of Transonic Flows in Diffusers. *AIAA Paper 81-1240,* june, 1981.

[10]M. Sajben and T. J. Bogar. Unsteady Transonic Flow in a Two-Dimensional Diffuser : Interpretation of Experimental Results. Report MDC Q0779, Mac Donnell Douglas Corp., March 1982.

[11]M. Sajben, T. J. Bogar, and J. C. Kroutil. Characteristic Frequency and Length Scales in Transonic Diffuser Flow Oscillations. *AIAA paper 81-1291,* june, 1981.

Appendix

- **One-dimensional theory**

To simplify the notations the following quantities $\tilde{\omega}$ and Ω are introduced :

$$\tilde{\omega} = \omega - k\bar{V} \quad \text{and} \quad \Omega = \sqrt{k^2(\bar{a}^2 - \bar{U}^2) - \tilde{\omega}^2}$$

The eigenvalues of $\mathbf{C^{-1}B}$ are:

$$l_1 = \frac{-i\tilde{\omega}\bar{U} + \bar{a}\Omega}{\bar{a}^2 - \bar{U}^2},\ l_2 = \frac{-i\tilde{\omega}\bar{U} - \bar{a}\Omega}{\bar{a}^2 - \bar{U}^2},\ l_3 = l_4 = \frac{i\tilde{\omega}}{\bar{U}}, \tag{29}$$

and the eigenvectors of these eigenvalues are :

$$\vec{V_1} = \begin{bmatrix} \frac{1}{C_p k}(i\bar{U}l_1 + \tilde{\omega}) \\ \frac{\bar{\rho}}{k\bar{a}}(i\bar{U}l_1 + \tilde{\omega}) \\ -\frac{1}{k\bar{U}}i\bar{U}l_1 \\ 1 \end{bmatrix}, \vec{V_2} = \begin{bmatrix} \frac{1}{C_p k}(i\bar{U}l_2 + \tilde{\omega}) \\ \frac{\bar{\rho}}{k\bar{a}}(i\bar{U}l_2 + \tilde{\omega}) \\ -\frac{1}{k\bar{U}}i\bar{U}l_2 \\ 1 \end{bmatrix},$$

$$\vec{V_3} = \begin{bmatrix} 1 \\ -\frac{\bar{\rho}}{\bar{T}} \\ 0 \\ 0 \end{bmatrix}, \vec{V_4} = \begin{bmatrix} 0 \\ 0 \\ 1 \\ -\frac{\tilde{\omega}}{k\bar{U}} \end{bmatrix}. \tag{30}$$

- **Two-dimensional theory**

The matrix expressions of partial differential system are :

$$C = \begin{pmatrix} 0 & \bar{U} & \bar{\rho} & 0 \\ r\bar{\rho} & r\bar{T} & \bar{\rho}\bar{U} & 0 \\ 0 & 0 & 0 & \bar{\rho}\bar{U} \\ C_p\bar{U}\bar{\rho} & 0 & \bar{\rho}\bar{U}^2 & \bar{\rho}\bar{U}\bar{V} \end{pmatrix} \tag{31}$$

$$D = \begin{pmatrix} 0 & \bar{V} & 0 & \bar{\rho} \\ 0 & 0 & \bar{\rho}\bar{V} & 0 \\ r\bar{\rho} & r\bar{T} & 0 & \bar{\rho}\bar{V} \\ C_p\bar{V}\bar{\rho} & 0 & \bar{\rho}\bar{U}\bar{V} & \bar{\rho}\bar{V}^2 \end{pmatrix} \tag{32}$$

$$\begin{pmatrix} 0 & a_{12} & -\frac{\partial\bar{\rho}}{\partial x} & -\frac{\partial\bar{\rho}}{\partial y} \\ -r\frac{\partial\bar{\rho}}{\partial x} & a_{22} & \bar{\rho}(i\omega - \frac{\partial\bar{U}}{\partial x}) & -\bar{\rho}\frac{\partial\bar{U}}{\partial y} \\ -r\frac{\partial\bar{\rho}}{\partial y} & a_{32} & -\bar{\rho}\frac{\partial\bar{V}}{\partial x} & \bar{\rho}(i\omega - \frac{\partial\bar{V}}{\partial y}) \\ i\omega C_v\bar{\rho} & -i\omega r\bar{T} & a_{43} & a_{44} \end{pmatrix} \tag{33}$$

with :

$$\begin{aligned} a_{12} &= i\omega - \frac{\partial\bar{U}}{\partial x} - \frac{\partial\bar{V}}{\partial y} \\ a_{22} &= -\bar{U}\frac{\partial\bar{U}}{\partial x} - \bar{V}\frac{\partial\bar{U}}{\partial y} - r\frac{\partial\bar{T}}{\partial x} \\ a_{32} &= -\bar{U}\frac{\partial\bar{V}}{\partial x} - \bar{V}\frac{\partial\bar{V}}{\partial y} - r\frac{\partial\bar{T}}{\partial y} \\ a_{43} &= (i\omega - \bar{U}\frac{\partial\bar{U}}{\partial x} - \bar{V}\frac{\partial\bar{U}}{\partial y})\bar{\rho} \\ a_{44} &= i\omega\bar{\rho}\bar{V} - \bar{\rho}\bar{U}\frac{\partial\bar{V}}{\partial x} - \bar{\rho}\bar{V}\frac{\partial\bar{V}}{\partial y} \end{aligned}$$

The vector and matrix expressions of algebraic system (18) are:

$$A = \begin{pmatrix} 0 & \bar{U}_1 & \bar{\rho}_1 & 0 \\ r\bar{\rho}_1 & \bar{U}_1 + r\bar{T}_1 & 2\bar{\rho}_1\bar{U}_1 & 0 \\ C_p & 0 & \bar{U}_1 & 0 \\ 0 & 0 & 0 & 1 \end{pmatrix} \tag{34}$$

$\xi = \xi_0 - \xi_1$ and $\eta = \eta_0 - \eta_1$ with :

$$\xi_i = \begin{pmatrix} \frac{\partial}{\partial x}(\bar{\rho}_i\bar{U}_i) + i\omega_i\bar{\rho}_i \\ \frac{\partial}{\partial x}(\bar{p}_i + \bar{\rho}_i\bar{U}_i^2) + 2i\omega_i\bar{\rho}_i\bar{U}_i \\ \frac{\partial}{\partial x}(C_p\bar{T}_i + \frac{1}{2}\bar{U}_i^2) + i\omega_i\bar{U}_i \\ \frac{\partial\bar{V}_i}{\partial x} \end{pmatrix} \tag{35}$$

$$\eta_i = \begin{pmatrix} -\bar{\rho}_i\bar{V}_i \\ -2\bar{\rho}_i\bar{U}_i\bar{V}_i \\ -\bar{U}_i\bar{V}_i \\ \bar{U}_i \end{pmatrix} \tag{36}$$